Optically detected electron-paramagnetic-resonance investigations of the substitutional oxygen defect in gallium arsenide

F. K. Koschnick, M. Linde, M. V. B. Pinheiro, and J.-M. Spaeth
University of Paderborn, Fachbereich Physik, D-33095 Paderborn, Germany
(Received 8 April 1997)

The substitutional oxygen defect in GaAs has been investigated with magnetic circular dichroism of the absorption, optically detected electron paramagnetic resonance, and optically detected electron-nuclear double resonance (ODENDOR). The ODENDOR spectra can be explained with an oxygen atom occupying an As site displaced from a regular lattice position along a ⟨100⟩ direction. The superhyperfine interactions and spin densities for several As and Ga neighbors have been determined. The experiments support a model in which the oxygen atom is bonded to two Ga atoms and which shows similarities to the *A* center in silicon. [S0163-1829(97)03339-0]

I. INTRODUCTION

The electrically active oxygen defect (O_{As}) in GaAs has become a matter of considerable interest in recent years. From local vibrational mode spectroscopy (LVM) it was suggested that an oxygen atom binds with two Ga atoms,[1] i.e., is displaced from a regular lattice position. Three different LVM-line groups belonging to three different charge states of the O_{As} (A, B, and B') were detected.[2] Recharging experiments have demonstrated the negative U character of this defect.[3] Similar experiments using magnetic resonance techniques revealed that the B' state is the paramagnetic one.[4] B' is a metastable state. In n-type GaAs only the diamagnetic ground state B is occupied upon cooling the sample in the dark.

Details of the microscopic and the electronic structure of the defect are not yet fully understood. In this paper, using optically detected electron-nuclear double resonance (ODENDOR) measurements the structural model for this defect is investigated and discussed. The ''off center'' model proposed from LVM is essentially confirmed and the superhyperfine (shf) interactions with many shells of lattice nuclei were determined. A preliminary account of the ODENDOR results were given in Ref. 5.

II. EXPERIMENTAL DETAILS

The investigated GaAs crystal was grown with the horizontal Bridgman technique in our laboratory using quartz crucibles. The sample was slightly n type and the position of the Fermi level was determined by temperature-dependent Hall-effect measurements to be 430 meV below the conduction-band edge. IR-absorption measurements showed strong LVM lines of the O_{As} defect. The magnetic circular dichroism of the absorption (MCDA), optically detected electron paramagnetic resonance (ODEPR), and ODENDOR measurements were performed in a K-band ($\nu = 24$ GHz) spectrometer. ODEPR was detected as a microwave-induced change of the MCDA. ODENDOR was measured as an increase of the ODEPR signal due to NMR transitions induced by rf. A cooled germanium detector was used to measure the transmitted light. The MCDA, which is the differential absorption of left and right circularly polarized light propagating along an external magnetic field, was determined in combination with a linear polarizer and an optical stress modulator via a lock-in technique.

In order to measure ODENDOR of the first Ga shell of O_{As} the frequency range of the rf system had to be extended to 400 MHz. This required considerable modification of our electron-nuclear double resonance (ENDOR) apparatus. Due to the cavity design, the two ENDOR coils have to be connected symmetrically to the rf source. However, commercial rf amplifiers have asymmetrical outputs with an impedance of 50 Ω. Another difficulty in achieving a good coupling of the rf output of the amplifier to the ENDOR coils at frequencies above 100 MHz is the length of the rf lines. The distance from the top of the cryostat to the ENDOR coils in the cavity is approximately 1.2 m. For frequencies above 100 MHz the length of the rf lines is of the order of the rf wavelength. This leads to a transformation of the impedance along the rf line resulting in a strong variation of the rf amplitude at the ENDOR coils. To avoid resonances of the rf system and to ensure a smooth and small variation of the rf amplitude when tuning the frequency, we symmetrized the rf line from the amplifier with a so-called balun, which was realized with a line transformer.[6] The two ENDOR coils in the cavity were connected with four coaxial lines with an impedance of 50 Ω to the balun. The rf setup showed no resonances due to impedance tranformations. In the low-frequency range the rf current is determined by the output impedance of the rf amplifier, and in the high-frequency range it is limited by the impedance of the ENDOR coils. (The inductivity of the coils is approximately 10 nH.)

For further experimental details the reader is referred to Ref. 7.

III. RESULTS

After cooling the sample in the dark, the well-known MCDA spectrum of $EL2^+$ is found (curve *a* in Fig. 1). Above 1.4 eV, an MCDA band of an unknown defect is superimposed on the MCDA of $EL2^+$ in this spectrum. The MCDA of the $EL2^+$ above 1.4 eV is represented by a dashed line.

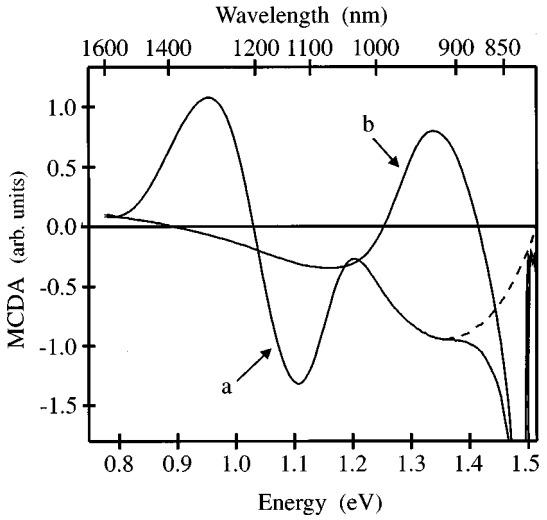

FIG. 1. (a) MCDA measured with normal light intensity at 1.5 K, B=2 T; (b) MCDA after illumination with 1.17 eV light (bleaching of $EL2$). The signal at 1.47 eV is due to an unknown defect.

It is surprising that this charge state of $EL2$, $EL2^+$, is measured considering the position of the Fermi level. This observation can be explained by considering that the sample is illuminated with light during the measurement, which results in optically induced recharging processes of the O_{As} charge states A, B, and B' (see Refs. 4, 8, and 5):

$$EL2^0+h\nu\rightarrow EL2^+ + e^-,\quad A+e^-\rightarrow B',\quad B'+e^-\rightarrow B. \tag{1}$$

After the bleaching of $EL2$ with light of 1.17 eV at 1.5 K a new MCDA signal appears (Fig. 1, curve b), which was previously correlated to the paramagnetic state B' of the O_{As} defect.[9] In this MCDA an ODEPR line can be detected (see Fig. 2). The halfwidth ($\Delta B_{1/2}$) of this EPR line is 90 mT and the value of the g factor is $g=2.01\pm0.005$. The line is isotropic within experimental error. The only isotope of oxygen with a nonzero nuclear spin (^{17}O, $I=5/2$) is only 0.038% abundant. Therefore, no hyperfine interaction with a central

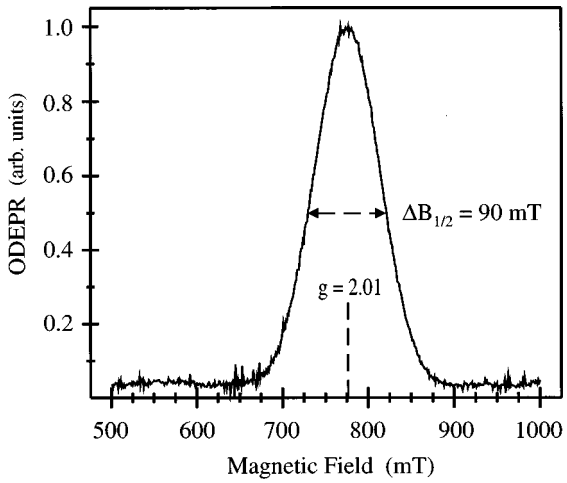

FIG. 2. ODEPR line of the O_{As} defect, measured at 1.32 eV after bleaching of $EL2$.

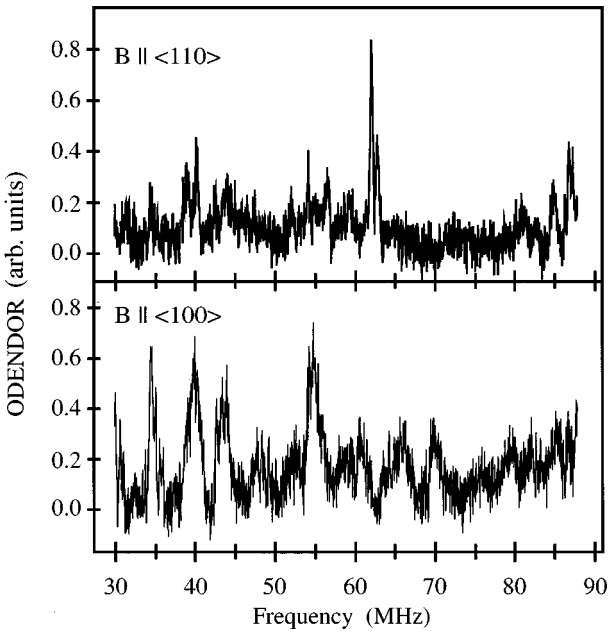

FIG. 3. ODENDOR-spectrum of the O_{As} defect for $B\|\langle100\rangle$ and $B\|\langle110\rangle$ measured in the center of the ODEPR line of Fig. 2.

nucleus is observed. The linewidth is of Gaussian shape and can be explained with unresolved shf interactions with the neighbor nuclei of the defect. To obtain more information about these interactions ODENDOR measurements were performed.

ENDOR lines were detected in the frequency range 30–90 MHz and 150–360 MHz. ODENDOR spectra in the 30–90 MHz range for $B\|\langle100\rangle$ and $B\|\langle110\rangle$, measured in the center of the ODEPR line, are shown in Fig. 3. A spectrum, measured in the high frequency range 150–360 MHz for the orientation $B\|\langle100\rangle$ can be seen in Fig. 4(a). The angular dependence of the ODENDOR lines was measured rotating the crystal about a [110] axis from $B_0\|[100](0°)$ via $B_0\|[111](54.74°)$ to $B_0\|[110](90°)$.

The frequency positions of the ODENDOR lines can be calculated using the following Hamiltonian:

$$\mathbf{H}=\underbrace{\mu_B g\vec{\mathbf{S}}\cdot\vec{\mathbf{B}}_0}_{ez}+\underbrace{\vec{\mathbf{I}}\cdot\underline{\underline{A}}\cdot\vec{\mathbf{S}}}_{shf}-\underbrace{g_N\mu_N\vec{\mathbf{I}}\cdot\vec{\mathbf{B}}_0}_{nz}+\underbrace{\vec{\mathbf{I}}\cdot\underline{\underline{Q}}\cdot\vec{\mathbf{I}}}_{q} \tag{2}$$

with ez the electron Zeeman energy, shf the superhyperfine interaction, nz the nuclear Zeeman energy, q the quadrupole interaction, A the superhyperfine (shf) tensor, Q the quadrupole tensor, $\underline{\underline{\mu}}_B$ the Bohr magneton, g the electron g value, $\vec{\mathbf{B}}_0$ the static magnetic field, $\vec{\mathbf{S}}$ the electron spin, $\vec{\mathbf{I}}$ the nuclear spin, μ_N the nuclear magneton, and g_N the nuclear g value. The frequencies for ENDOR transitions (selection rules for ENDOR: $\Delta m_I=\pm1$ and $\Delta m_S=0$) in a first-order solution of the Hamiltonian with an electron spin of $S=1/2$ are given by

$$\Delta\nu^{\pm}=\frac{1}{h}\left|\tfrac{1}{2}W_{\mathrm{shf}}\mp m_q W_q\pm g_n\mu_n B_0\right| \tag{3}$$

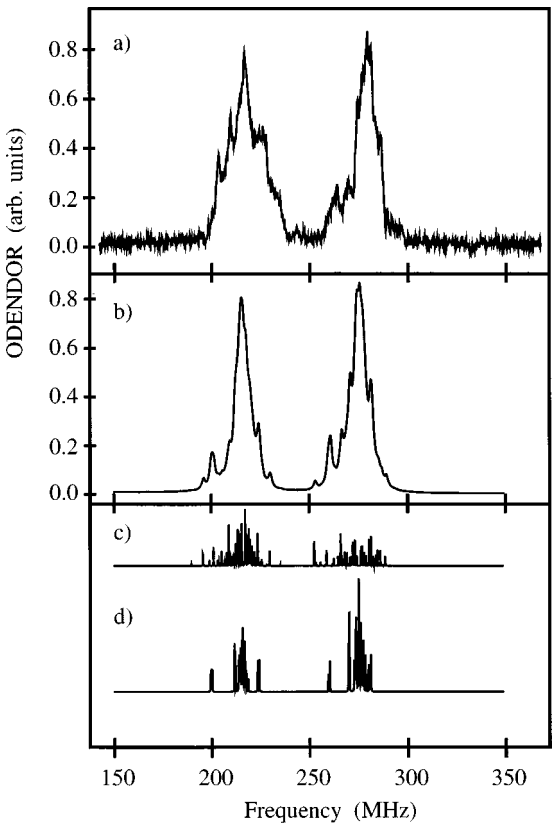

FIG. 4. (a) ODENDOR spectrum of the first Ga shell of the O_{As} defect for $B\|\langle 100\rangle$, $B_0=875$ mT; (b) calculated spectrum with the parameters from Tables I, II, and III; (c) and (d) stick spectra of the calculated ODENDOR lines, the relative line intensities consider the transition probabilities and the abundances of the two Ga isotopes; in (c) the ^{69}Ga-^{69}Ga (lower-frequency range) and the ^{71}Ga-^{71}Ga isotope combination are shown; in (d) the mixed isotope combination is presented.

with

$$W_{\rm shf}=a+b(3\cos^2\Theta-1)+b'\sin^2\Theta\cos(2\delta),$$

$$W_q=3q(3\cos^2\Theta'-1)+q'\sin^2\Theta'\cos(2\delta'),$$

$$m_q=\tfrac{1}{2}(m_I+m_{I'}). \qquad (4)$$

$m_I, m_{I'}$ are the magnetic quantum numbers of the levels associated with the ENDOR transitions. $W_{\rm shf}$ is given in terms of the isotropic shf interaction constant a, the anisotropic shf interaction constants b and b'. b' is related to the deviation of the shf tensor from axial symmetry. For the quadrupole interaction, the parameters q and q' are used. The shf interaction and the quadrupole parameters are related to the principal values of the shf and quadrupole tensors $\underline{\underline{A}}$ and $\underline{\underline{Q}}$ by $A_{xx}=a-b+b', A_{yy}=a-b-b', \quad A_{zz}=a+2b$ and $Q_{xx}=-q+q', Q_{yy}=-q-q', Q_{zz}=2q$. Θ, δ, Θ', and δ' are the polar angles of the magnetic field with respect to the principal axis systems of the shf and quadrupole tensor, respectively. ν^+ is the sum frequency where $m_S=-\frac{1}{2}$ and ν^- is the difference frequency where $m_S=+\frac{1}{2}$.

The signal-to-noise ratio of the measured ENDOR lines was very low, and it was difficult to follow a certain ODENDOR line through the full angular dependence. Another problem, which complicated the analysis, was the overlap of many lines. In particular, a superposition of many ODENDOR lines was observed in the high-frequency range [Fig. 4(a)]. The first step in the evaluation of the ENDOR data was to determine the chemical nature of the nuclei producing the ODENDOR lines. It can be seen from Eq. (3) that a specific ENDOR line will shift if the magnetic field is changed. Since the resonance condition for the EPR transition has to be fulfilled to measure ODENDOR, the magnetic field can only be varied within the EPR linewidth. The chemical nature of nuclei giving rise to the ODENDOR lines (^{69}Ga, 60.1% abundance; ^{71}Ga, 39.9%; ^{75}As, 100%) could thus be determined by observing the shift of ENDOR lines as a function of the magnetic field (for details see Ref. 7). Because of the large width of the ODEPR line, these magnetic-field-shift experiments could be performed in the field range 820–910 mT. Examples of field-shift experiments are shown in Fig. 5.

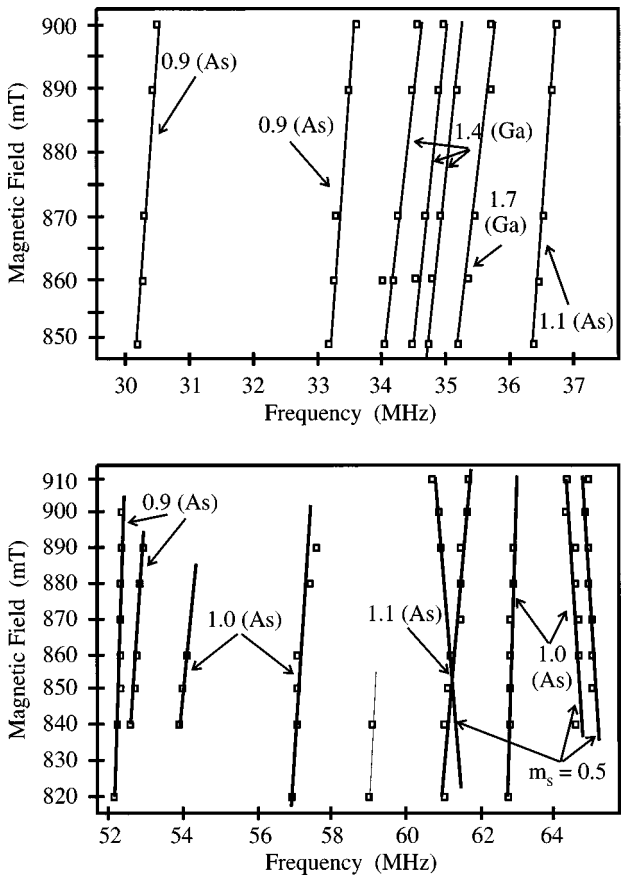

FIG. 5. Magnetic-field-shift experiments for ODENDOR lines in the intermediate frequency region, the isotopes identified from the shift are labeled. The error in the determination of the frequency positions of the ODENDOR lines is approx. 0.1 MHz.

The lines with the highest shf interactions (frequency range 150–360 MHz) are due to Ga neighbors. This can also be seen from the ratio of the frequency positions of the two groups of lines in Fig. 4(a), which is exactly the same ratio as that of the nuclear g values g_N of the two isotopes [$g_N(^{71}\text{Ga})/g_N(^{69}\text{Ga}) = 1.27$]. From the positive slope of the field shift of the ENDOR lines, it could be inferred that only the $m_S=-\frac{1}{2}$ branch (the so-called ''sum'' frequency) was measured (assuming that $W_{\rm shf}>0$). It is often observed that only the sum frequency can be detected with ENDOR for a

certain neighbor shell. The complex relaxation behavior of the electron-nuclear spin system is probably responsible for this effect.

ENDOR lines of Ga neighbors were also found at lower frequencies ($<$ 45 MHz). The lines in the intermediate range (50–90 MHz) are due to ^{75}As interactions. No lines due to oxygen isotopes were observed, as the only oxygen isotope with a nuclear spin (^{17}O) has a natural abundance of 0.038%.

For the structural analysis of the oxygen defect, the ODENDOR spectrum in the high-frequency range [see Fig. 4(a)] is very important. It yields information about the nearest (first) Ga shell and, therefore, information about the symmetry of the defect.

From Fig. 4(a), we estimated W_{shf} in first order [Eq. (3)] of this Ga shell for the $\langle 100 \rangle$ direction of the magnetic field. This first-order estimation was without any assumptions of the symmetry. If the magnetic field is parallel to the $\langle 100 \rangle$ direction, the shf interaction was determined to be 410 MHz and 520 MHz for ^{69}Ga and ^{71}Ga, respectively. If we assume an on-center position of the oxygen, then the first Ga shell consists of four Ga atoms. The linewidth of an inhomogeneously broadened EPR line of a paramagnetic defect can be calculated using the shf interactions of the neighbor nuclei (see, e.g., Ref. 7). For the linewidth calculation we only took into account the shf interactions estimated above, and we assumed four nuclei for the Ga shell. The result is represented by the stick spectrum of Fig. 6(b). In order to obtain a smooth envelope curve of the calculated ODEPR line, a minimum width of 30 mT was chosen for each individual line, since the measured ODEPR line (see Fig. 2) also does not show any structure. The additional broadening of the EPR line from higher shells is taken into account with the individual linewidth. The half-width of the calculated EPR line, assuming four equivalent Ga nuclei and taking the smallest individual linewidth of 30 mT, which avoids shf structure in the ODEPR line, is 100 mT [full width at half maximum (FWHM) see enevelope in Fig. 6(b)]. This value is the lowest limit of the half-width under the assumption of four equivalent Ga neighbors. It is too large compared with the measured linewidth of 90 mT (see Fig. 2). The assumption of three equivalent Ga nuclei in the first shell gives a minimum halfwidth of approximately 95 mT, which is also too large. Therefore, we rule out that the first Ga shell consists of three or four equivalent Ga nuclei. In Fig. 6(a) the result for two nuclei in the first Ga shell is given. The linewidth in this case is 80 mT. In this calculation, the individual linewidth was increased to 35 mT to avoid any structure. The value of 80 mT is the minimum ODEPR linewidth expected for two equivalent Ga nuclei in the first Ga shell. It must be pointed out that we do not know the exact value of the individual linewidth at this stage of analysis and that we can calculate an ODEPR linewidth of 90 mT with two equivalent Ga nuclei assuming a larger individual linewidth than 35 mT. Thus, we conclude that the first Ga shell consists of two nuclei.

For the ENDOR analysis, we make the following assumptions justified by the linewidth discussion above.

The first Ga shell consists of two nuclei. Therefore, the oxygen impurity must occupy an off-center position along a $\langle 100 \rangle$ direction. In such a case, the nearest Ga neighbor shell for tetrahedral symmetry splits into two monoclinic sub-

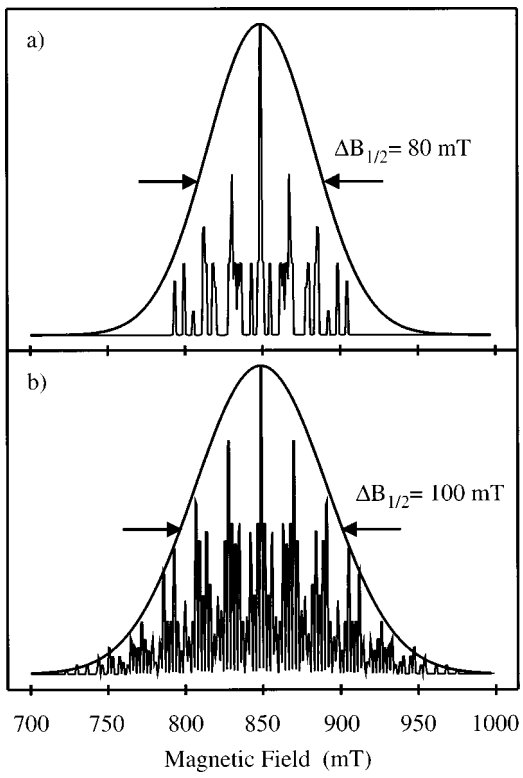

FIG. 6. Calculated linewidth of the EPR with the shf interaction of the first Ga shell estimated in first order. In (a) it was assumed that the first Ga shell consists of two equivalent nuclei, in (b) we assumed four equivalent Ga nuclei. The stick spectra represent the positions of the individual shf-split EPR lines arising from the interaction with the first Ga shell. The broad lines that envelope the stick spectra represent the convolution of the individual lines with Gaussians. The half-width of the Gaussians were chosen to be just large enough to prevent a structure on the envelope curve. For further details see text.

shells, each consisting of two Ga nuclei. Therefore, it is expected that the shell with the highest shf interactions is a Ga shell as measured. Because of the off-center position of the oxygen, the defect symmetry is orthorhombic. This leads to six center orientations, each along a $\langle 100 \rangle$ direction. In Fig.

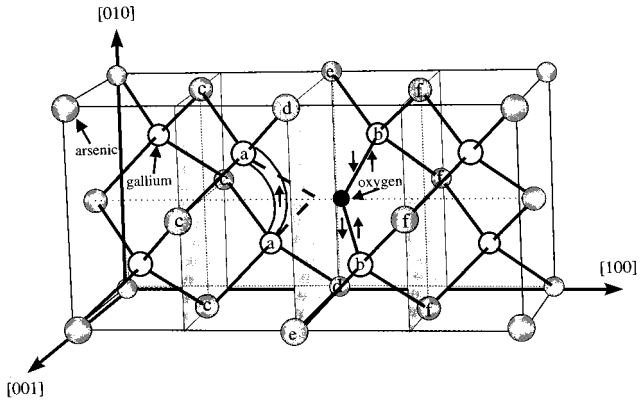

FIG. 7. Nearest Ga and As shells for the orthorhombic O_{As} defect. The unpaired spin of the paramagnetic B' charge state is located in the rebonded dangling bond between the two Ga atoms of the first Ga shell.

TABLE I. shf interactions of the nearest-neighbor shells, (a)–(f) refer to positions in Fig. 7.

Shell	a/h (MHz)	b/h (MHz)	b'/h (MHz)	Symmetry
1. ^{69}Ga shell (a)	402	57		monoclinic
2. ^{69}Ga shell (b)	54.9	5.1	1.7	monoclinic
1. ^{75}As shell (d)	135	8.5	1	monoclinic
2. ^{75}As shell (c)	122	18	−7	triclinic
3. ^{75}As shell (e)	95	5	2	monoclinic
4. ^{75}As shell (f)	45	5.5	−5	triclinic

7 the model for the off-center position of the oxygen in GaAs is shown. Also indicated are the different subshells of Ga and As neighbor nuclei. The symmetries of these subshells were taken into account for the ENDOR analysis.

In Fig. 4(b) the calculated ODENDOR spectrum for $B\|\langle 100\rangle$ with the shf and quadrupole interaction parameters from Tables I, II, and III (first Ga shell) is shown. This spectrum was calculated assuming a monoclinic Ga shell consisting of two Ga atoms and the two isotopes ^{69}Ga and ^{71}Ga both with $I=3/2$. The frequency positions of the individual ODENDOR lines are illustrated in Fig. 4 (stick spectra c and d). The spectrum is a complicated superposition of many ODENDOR lines. In the stick spectrum c of Fig. 4 the isotope combinations ^{69}Ga-^{69}Ga (lower frequency) and ^{71}Ga-^{71}Ga (higher frequency) are shown for the two nuclei. The mixed isotope combination ^{69}Ga-^{71}Ga can be seen in stick spectrum d of Fig. 4. The relative intensities of the lines for these three isotope combinations due to their natural abundance is 2.25 : 3.0 : 1.0 for ^{69}Ga-^{69}Ga : ^{69}Ga-^{71}Ga : ^{71}Ga-^{71}Ga, respectively. The calculated spectrum (Fig. 4, curve b, the details of the calculation are presented below) is a superposition of the three combinations assuming a linewidth of 1 MHz for each ODENDOR transition. This width is a reasonable value for the ODENDOR lines in GaAs (see Fig. 3 and also, for example, Ref. 10). The overall agreement with the experimental spectrum is satisfactory.

For the calculation of the stick spectra, neither Eq. (3) nor the effective spin approximation where the electron spin operator in the Hamiltonian [Eq. (2)] is replaced by the effective electron spin and the nuclear spins are assumed to be independent from each other, is sufficient. In the effective spin treatment of the Hamiltonian, the diagonalization is only performed for the ''reduced'' nuclear spin matrices. Because of the large shf interactions of the Ga nuclei with the electron spin (about 400 MHz), the full matrix including the electron spin and the nuclear spins of the spin Hamiltonian had to be diagonalized. The large shf interactions of the Ga nuclear spins lead to three effects: One effect is the so-called pseudodipolar splitting due to the indirect interaction between magnetically equivalent nuclear spins via the electron spin.[11] The splittings of the ENDOR lines in the calculated spectrum (Fig. 4, stick spectrum c) are essentially due to the pseudodipolar coupling. The second effect is a splitting, which looks like a quadrupole splitting. It is caused by the influence of a nuclear spin on the quantization axis of the electron spin with which it is interacting. The nuclear spins need not be magnetically equivalent. Therefore, the splitting is also present for the ^{69}Ga-^{71}Ga isotope combination (see Fig. 4, stick spectrum d). The third effect is the occurrence of nuclear spin transitions where more than one nuclear spin flips or where $|\Delta m_I|>1$ (forbidden transitions). The probability of these transitions may be increased dramatically with a larger shf interaction.

TABLE II. Orientations of the shf tensors of the nearest-neighbor shells in terms of the Euler angles. β is the angle between the z axis of the shf tensor and the $\langle 100\rangle$ direction along which the oxygen atom is displaced. The z and the x axes of the shf tensors of the monoclinic shells must be located in the [110] plane that contains the two neighbor nuclei of that shell. Therefore, the angles α and γ of these shells are not free parameters.

Shell	α (degrees)	β (degress)	γ (degrees)	Symmetry
1. ^{69}Ga shell	0	56.5	45	monoclinic
2. ^{69}Ga shell	0	62	45	monoclinic
1. ^{75}As shell	0	43	45	monoclinic
2. ^{75}As shell	25	65	50	triclinic
3. ^{75}As shell	0	46	45	monoclinic
4. ^{75}As shell	35	75	50	triclinic

The matrix of the spin Hamiltonian for one of the isotope combinations has a dimension of 32 (two nuclear spins of 3/2 and one electron spin of 1/2). The matrix consists of two subsystems for each m_S branch. Within such a subsystem with a dimension of 16, ENDOR transitions are possible. That leads to a number of $\binom{16}{2}=120$ transitions for each subsystem and each of the three isotope combinations. Because we only measured the sum frequency (see above), we have to consider 360 transitions. From our calculations, it turned out that approximately two-thirds of these lines have a negligible transition probability. Therefore, the ODENDOR spectrum in Fig. 4 is a superposition of approximately 120 lines.

First, the shf and quadrupole parameters of the first Ga shell were estimated by a least-squares fit of the angular dependence of the ODENDOR lines with the approximation of an effective electron spin.[7] Then the parameter were determined by the ''best'' fit of the calculated spectrum to the experimental spectrum with the full diagonalization of the Hamiltonian.

The As lines between 50 and 70 MHz cannot be described by only one As neighbor shell. Three As shells must be assumed in order to satisfactorily explain the number of As lines. The shf interactions of these shells turn out to be rather similar. The assumption of a paramagnetic oxygen on a tetrahedral symmetry As site would lead to a first As shell of 12 neighbors, a second shell of 6 neighbors, and a third shell of

TABLE III. Quadrupole parameter of the first Ga shell for the isotope ^{69}Ga. The angles marked with an asterisk are determined by symmetry. The z and x axis of the quadrupole tensor must be located in the [110] plane which contains the two Ga nuclei. β is the angle between the z axis of the quadrupole tensor and the $\langle 100\rangle$ direction along which the oxygen atom is displaced.

q/h (MHz)	q'/h (MHz)	α (degrees)	β (degrees)	γ (degrees)
1.6		0*	8	45*

TABLE IV. Neighbor shells for a defect on an arsenic lattice site (tetrahedral symmetry).

	Number of nuclei in a shell	Distance (Å)
1. Ga shell	4	2.44
1. As shell	12	3.95
2. Ga shell	12	4.67
2. As shell	6	5.61
3. Ga shell	12	6.13
3. As shell	24	6.85

24 neighbors (see Table IV). However, the distances of the second and third shell compared to the first shell are too large to explain three shf interactions with only a 30% spread in values (i.e., 95–135 MHz). For a deep-level defect the spin density roughly falls off exponentially with distance. This observation again points to the off-center position of the oxygen as concluded from the first Ga shell. In such a case, the nearest As shell splits into four subshells (two with monoclinic and two with triclinic symmetry). The ENDOR lines were explained assuming this configuration. In Tables I and II, the values of the shf interaction parameters of all measured shells, obtained from the ENDOR analysis, are collected. No quadrupole splitting was observed for any As shell or the second Ga shell.

Using the shf parameters for all measured shells, the EPR linewidth was calculated again. The resulting half-width with two Ga nuclei in the first Ga shell is now 89 mT. This is in very good agreement with the measured width of 90 mT and shows that a large shf interaction was not overlooked. With the assumption of three and four Ga nuclei in the first shell we obtained 102 mT and 115 mT, respectively, which is definitely too large. Therefore, our ENDOR results confirm the model proposed from LVM measurements.[3]

With the exception of the first Ga shell, no quadrupole interactions were observed. A rough estimate for the quadrupole interaction of the nearest As neighbors, caused by a point charge, is given by the following equation (see, e.g., Ref. 7):

$$q=\frac{e^2Q(1-\gamma_\infty)}{2I(2I-2)4\pi\epsilon_0R^3}. \tag{5}$$

Q is the quadrupole moment of the nucleus, e is the elemental charge, ϵ_0 is the electrical field constant, R is the distance of the nucleus from the point charge, and $(1-\gamma_\infty)$ is the Sternheimer antishielding factor for a charge outside the core of the atom. $(1-\gamma_\infty)$ is 40 for As.[12] For a point charge of 1, a value of approximately 1 MHz is calculated for the first As shell. A quadrupole interaction of this magnitude was not observed for the As shells, but would have been resolved, if present. Therefore, the defect must be in a neutral charge state. The quadrupole interaction of the first Ga shell can be explained with an electric-field gradient arising from the unpaired spin density moving in a p orbital only:[13]

$$q=\frac{Se^2Q(1-\gamma)}{2I(2I-2)\epsilon_0\mu_0g_eg_N\mu_B\mu_N}b(P_\sigma). \tag{6}$$

$(1-\gamma)$ is the atomic antishielding factor, which is not known and which is expected to be approximately 1. μ_0 is the magnetic induction constant, S is the electron spin, and $b(P_\sigma)$ is the anisotropic shf parameter after deduction of the point dipole-dipole contribution b_{dd} (1 MHz for the first ^{69}Ga shell). An estimate of the quadrupole interaction parameter q for the ^{69}Ga isotope of the first Ga shell using Eq. (6) and with $b(P_\sigma)=56$ MHz gives 1.4 MHz, which is very close to the measured value of 1.6 MHz. For the arsenic shells, the quadrupole interaction arising from the unpaired spin density moving in a p orbital is too small to be resolved.

IV. DISCUSSION

An off-center model for the O_{As} defect similar to the off-center model for oxygen in silicon (A center[14]) was proposed by Refs. 3 and 15. Figure 7 shows the neutral charge state in this model. If an As atom is removed from its lattice position, three electrons are left in the dangling bonds of the remaining vacancy. If an O atom is added, two of the electrons are required for the Ga-O-Ga bonding. It is supposed that this bonding is quite stable. The remaining electron is located in the rebonded dangling bonds. This state is paramagnetic. No large quadrupole interaction for such a paramagnetic defect is expected, because this state is neutral with respect to the lattice. The neutral state is the B' state. In qualitative agreement with this model we observe a very large Ga interaction, which contains the largest fraction of the unpaired spin density and several subshells of nearest As neighbors with comparable interactions. The A state is the state where the unpaired electron is removed; the B state is the one where the rebonded dangling bond is occupied by two electrons [negative U, since this is the ground state (Ref. 3)].

An approximation for the spin-density distribution of a deep defect can be found with a linear combination of atomic orbitals (LCAO) approximation (see, e.g., Ref. 14):

$$\Psi=\Psi_0+\sum_i \eta_i\Psi_i. \tag{7}$$

Ψ is the wave function of the defect, Ψ_0 is the wave function of the central atom if present, and the Ψ_i are the wave functions at the neighbor atoms of the defect. A hybridized orbital in GaAs can be expressed as

$$\Psi_i=\alpha_i(\Psi_{4s})_i+\beta_i(\Psi_{4p})_i. \tag{8}$$

The following conditions of normalization must hold: $\Sigma_i\eta_i^2=1$ and $\alpha_i^2+\beta_i^2=1$. η_i^2 is the spin density at the neighbor i. $\eta_i^2\alpha_i^2=a_i/a_f$ is the s-like and $\eta_i^2\beta_i^2=b_i/b_f$ the p-like density. a_f and b_f are the shf parameters for the free atoms as, for example, calculated by Ref. 16. With a_f(As)= 14660 MHz, a_f(^{69}Ga) = 12210 MHz, b_f(As) = 334 MHz, and b_f(^{69}Ga) = 204 MHz (Ref. 16) the values of Table V were calculated. For nearly all the shells an sp^3 character is found. Within this simple model, we account for about 100% of the spin density with the measured shells. The majority of the unpaired spin density (60%) is located on the first Ga shell. At the two Ga atoms to which the oxygen is bound (second Ga shell), only one-tenth of that amount is located. It is interesting to compare the spin density for different As

TABLE V. Distribution of the spin density on the nearest neighbors; n is the number of nuclei in a shell, (a)–(f) refer to positions in Fig. 7.

Shell	α^2	β^2	η^2	n	$n\eta^2$
1.Ga shell (a)	0.1	0.9	0.3	2	0.6
2. Ga shell (b)	0.15	0.85	0.03	2	0.06
1. As shell (d)	0.27	0.73	0.03	2	0.06
2. As shell (c)	0.14	0.86	0.06	4	0.24
3. As shell (e)	0.30	0.70	0.02	2	0.04
4. As shell (f)	0.16	0.84	0.02	4	0.08
				Σ	1.08

shells. The second As shell (labeled c in Fig. 7), which is close to the first Ga shell (labeled a in Fig. 7), has a much larger spin density than the fourth As shell (labeled f in Fig. 7). It has even a larger spin density than the first As shell (labeled d in Fig. 7). The reason for this is probably a transfer of spin density to the second As shell via the Ga atoms of the first Ga shell.

V. CONCLUSIONS

With our ODENDOR analysis of the B' state of the substitutional oxygen defect O_{As}, we could show that the oxygen has an off-center position. It is moved along a $\langle 100 \rangle$ direction. Therefore, the defect has orthorhombic symmetry. Our results confirm a recent LVM study of O_{As}.[3] Because we did not observe considerable quadrupole splittings for the As shells, we concluded that the paramagnetic B' state is the neutral charge state of the O_{As} defect in agreement with previous magneto-optical studies.[4] Our results confirm the model proposed by Refs. 3 and 15. In addition, we could estimate the spin-density distribution of the unpaired electron spin of the B' state for the first and second Ga shell and for four As shells. The spin density is accounted for very well within the LCAO approximation.

ACKNOWLEDGMENTS

This work was supported by the Deutsche Forschungsgemeinschaft. We are grateful for the technical assistance of K.-H. Wietzke for the improvement of the rf system of our ODENDOR spectrometer.

[1] J. Schneider, B. Dischler, H. Seelewind, P. M. Mooney, J. Lagowski, M. Matsui, D. R. Beard, and R. Newman, Appl. Phys. Lett. **54**, 1442 (1989).
[2] H. Ch. Alt, Appl. Phys. Lett. **54**, 1445 (1989).
[3] H. Ch. Alt, Phys. Rev. Lett. **65**, 3421 (1990).
[4] M. Linde, J.-M. Spaeth, and H. Ch. Alt, Appl. Phys. Lett. **67**, 662 (1995).
[5] M. Linde, H. Ch. Alt, and J.-M. Spaeth, Mater. Sci. Forum **196-201**, 213 (1995).
[6] D. Nuehrmann, *Das grosse Werkbuch Elektronik* (Franzis Verlag, Poing, 1994).
[7] J.-M. Spaeth, J. R. Niklas, and R. H. Bartram, *Structural Analysis of Point Defects in Solids*, edited by M. Cardona, P. Fulde, K. von Klitzing, and H.-J. Queisser, Springer Series in Solid-State Sciences Vol. 43 (Springer-Verlag, Berlin, 1992).
[8] H. Ch. Alt, Semicond. Sci. Technol. **6**, B121 (1990).
[9] M. Jordan, M. Linde, Th. Hangleiter, and J.-M. Spaeth, Semicond. Sci. Technol. **7**, 731 (1992).
[10] J.-M. Spaeth and K. Krambrock, Adv. Solid State Phys. **33**, 111 (1993).
[11] T. E. Feuchtwang, Phys. Rev. **126**, 1628 (1962).
[12] D. Gill and N. Bloembergen, Phys. Rev. **129**, 2398 (1963).
[13] J. Owen and J. H. M. Thornley, Rep. Prog. Phys. **29**, 675 (1966).
[14] G. D. Watkins and J. W. Corbett, Phys. Rev. **121**, 1001 (1961).
[15] M. Skowronski, in *Deep Centers in Semiconductors*, edited by S. T. Pantelides (Gordon and Breach Scientific Publishers, Yverdon, Switzerland, 1992), Chap. 4.
[16] J. R. Morton and K. F. Preston, J. Magn. Reson. **30**, 577 (1978).